J Neurophysiol 118: 2296–2310, 2017.
First published July 19, 2017; doi:10.1152/jn.00321.2017.

RESEARCH ARTICLE | *Control of Movement*

Intra- and intersegmental influences among central pattern generating networks in the walking system of the stick insect

Charalampos Mantziaris,[1] Till Bockemühl,[1] Philip Holmes,[2] Anke Borgmann,[1] Silvia Daun,[1,3] and Ansgar Büschges[1]

[1]*Department of Animal Physiology, Zoological Institute, Biocenter, University of Cologne, Cologne, Germany;* [2]*Department of Mechanical and Aerospace Engineering, Program in Applied and Computational Mathematics and Princeton Neuroscience Institute, Princeton University, Princeton, New Jersey; and* [3]*Institute of Neuroscience and Medicine (INM-3), Forschungszentrum Jülich, Jülich, Germany*

Submitted 2 May 2017; accepted in final form 17 July 2017

Mantziaris C, Bockemühl T, Holmes P, Borgmann A, Daun S, Büschges A. Intra- and intersegmental influences among central pattern generating networks in the walking system of the stick insect. *J Neurophysiol* 118: 2296–2310, 2017. First published July 19, 2017; doi:10.1152/jn.00321.2017.—To efficiently move around, animals need to coordinate their limbs. Proper, context-dependent coupling among the neural networks underlying leg movement is necessary for generating intersegmental coordination. In the slow-walking stick insect, local sensory information is very important for shaping coordination. However, central coupling mechanisms among segmental central pattern generators (CPGs) may also contribute to this. Here, we analyzed the interactions between contralateral networks that drive the depressor trochanteris muscle of the legs in both isolated and interconnected deafferented thoracic ganglia of the stick insect on application of pilocarpine, a muscarinic acetylcholine receptor agonist. Our results show that depressor CPG activity is only weakly coupled between all segments. Intrasegmental phase relationships differ between the three isolated ganglia, and they are modified and stabilized when ganglia are interconnected. However, the coordination patterns that emerge do not resemble those observed during walking. Our findings are in line with recent studies and highlight the influence of sensory input on coordination in slowly walking insects. Finally, as a direct interaction between depressor CPG networks and contralateral motoneurons could not be observed, we hypothesize that coupling is based on interactions at the level of CPG interneurons.

NEW & NOTEWORTHY Maintaining functional interleg coordination is vitally important as animals locomote through changing environments. The relative importance of central mechanisms vs. sensory feedback in this process is not well understood. We analyzed coordination among the neural networks generating leg movements in stick insect preparations lacking phasic sensory feedback. Under these conditions, the networks governing different legs were only weakly coupled. In stick insect, central connections alone are thus insufficient to produce the leg coordination observed behaviorally.

motor control; locomotion; pilocarpine; coordination; phase coupling

ANIMALS MOVE VIA COORDINATED action of their trunk muscles and appendages: body segments and fins for swimming, wings for flying, and legs for walking. Irrespective of the mode of locomotion, underlying rhythmic motor activity is generated by specialized neural networks located anatomically close to the muscles they control (for overview, see Orlovsky et al. 1999). Central pattern generators (CPGs), neural circuits that can generate rhythmic motor activity in the absence of phasic input, are core elements of these networks (Katz and Hooper 2007; Marder and Bucher 2001; Marder and Calabrese 1996; Smith et al. 2013). Proper intra- and intersegmental coupling between CPGs is essential for limb coordination and adaptive motor control.

Insects generate different interleg coordination patterns during walking, depending on their behavioral task and locomotion speed (Bender et al. 2011; Cruse 1990; Grabowska et al. 2012; Mendes et al. 2013; Wendler 1964; Wosnitza et al. 2013). The number of legs simultaneously in swing phase increases with walking speed, allowing insects to express a continuum of walking patterns ranging from "wave gait" at low speeds (Graham 1985; Hughes 1952; Wosnitza et al. 2013) to tetrapod and tripod coordination patterns at higher speeds (Berendes et al. 2016; Hughes 1952; Mendes et al. 2013; Wilson 1966; Wosnitza et al. 2013). Thus there is great flexibility in intersegmental phase relationships between oscillatory neural networks that control leg movement, and these phase relationships vary between high and low walking speeds. However, information on the underlying mechanisms and the relative contribution of central and peripheral signaling in CPG coupling and interlimb coordination in insects remains highly elusive.

To induce centrally generated fictive motor activity in insects, the muscarinic acetylcholine receptor agonist pilocarpine has been commonly applied to deafferented invertebrate nerve cord preparations. Pharmacologically induced motor activity in the locust (Ryckebusch and Laurent 1993, 1994), the hawk moth (Johnston and Levine 2002), and the cockroach (Fuchs et al. 2011, 2012) have revealed approximately constant phase relationships between motor outputs of different segmental CPGs that closely resemble those observed in a tripod coordination pattern. In line with these studies, David et al. (2016) have recently proposed a connectivity model that attempts to account for this fictive tripod-like coordination, thereby em-

Address for reprint requests and other correspondence: A. Büschges, Dept. of Neurobiology/Animal Physiology, Biocenter, University of Cologne, Room 1.610, Zülpicher Straße 47b, 50674 Cologne, Germany (e-mail: ansgar.bueschges@uni-koeln.de).

phasizing the importance of central connectivity in coordination. In contrast, a recent study reported a tendency for in-phase activity between homologous motoneuron (MN) pools in the isolated and deafferented thoracic nerve cord of the locust (Knebel et al. 2017). This activity pattern did not resemble any of the known walking interleg coordination patterns in insects. Some indications for in-phase intersegmental coordination between homologous MNs have been published for the stick insect as well (Büschges et al. 1995). This discrepancy between species highlights potential differences in intersegmental information transfer between CPGs in the walking system of fast- and slow-walking animals and indicates the need to unravel the role of central connections in interleg coordination.

In the present study, we used the stick insect *Carausius morosus*, an exceptional animal model to study coordination as it is a nocturnal, slow-walking insect that inhabits highly variable environments, shows only minor functional differences between legs, and its locomotor behavior has been thoroughly investigated (Cruse 1990; Grabowska et al. 2012; Graham 1985; Wendler 1966). Its central nervous system (CNS) shares neuroanatomical and morphological characteristics with other invertebrate and vertebrate CNSs (Smarandache-Wellmann 2016). The MN pools driving the muscles of each leg joint are independently controlled by individual CPGs, located in the respective hemisegment of the ventral thoracic nerve cord (Bässler and Wegner 1983; Büschges et al. 1995). The mechanisms underlying the neural control of single-leg stepping in the stick insect have been extensively studied (Bässler and Wegner 1983; Büschges et al. 2008; Graham 1985), and the role of sensory feedback signals in intersegmental coordination has been well established (Borgmann et al. 2007, 2009; Cruse 1990; Cruse and Knauth 1989). However, the potential role of central neural interactions in interleg coordination during walking and the underlying neural mechanisms have never been addressed.

For the first time here, we applied a comprehensive phase analysis of pharmacologically induced, long-term rhythmicity in the stick insect. We show that, in the absence of sensory input, segmental CPGs controlling the movement of homologous muscles of the stick insect are only weakly phase coupled. We report intersegmental phase relationships that cannot account for the generation of any of the known interleg coordination patterns observed in the stick insect. Furthermore, we found no direct influence of CPGs on contralateral MN activity that would account for the weak interactions we observed. Thus we conclude that the weak central CPG interactions observed in the stick insect may add to the flexibility these animals need for interleg coordination when they move through their heterogeneous natural habitat.

MATERIALS AND METHODS

Animals

We used adult female stick insects of the species *Carausius morosus*. The animals were bred in-house in our colony and maintained at 22–24°C at ~60% humidity and under a 12:12-h light-dark cycle. The following experimental procedures comply with the German National and State Regulations for Animal Welfare and Animal Experiments.

Preparation

The experimental setup was based on established procedures (Büschges et al. 1995). CPG activity was assessed by recording rhythmic MN activity in the isolated and deafferented thoracic nerve cord after bath application of 5–7 mM of pilocarpine (Büschges et al. 1995). This concentration ensured activation and stable rhythmicity of MN pools in all segmental ganglia, a prerequisite for the subsequent analysis (Büschges et al. 1995). CPG coordination was analyzed within each deafferented thoracic ganglion (intrasegmental) while isolated (connective nerves were cut anteriorly and posteriorly to the ganglion) or connected to other thoracic ganglia of the isolated and deafferented thoracic nerve cord. To prevent peripheral sensory input from influencing the motor activity, we either pinched or cut all lateral nerves at the ganglia of interest.

Electrophysiological Recordings

Previous investigations (Büschges 1995; Büschges et al. 1995) have shown that pilocarpine-induced rhythmic activity in levator and depressor trochanteris MN pools consistently alternates, thus allowing us to monitor rhythmicity in these MN pools by exclusively recording and analyzing the activity of the depressor MNs. We focused on the coxa-trochanter (CTr) joint, because the activity of the muscles controlling movement of the CTr joint defines the stance and swing phases of each leg's stepping cycle, irrespective of the walking direction and orientation of locomotion (Rosenbaum et al. 2010). Moreover, there are only two excitatory MNs innervating the depressor trochanteris muscle in each hemisegment, a slow (SDTr) and a fast (FDTr) MN, a fact that increased the accuracy of our analysis. Lastly, there is a plethora of publications focusing on MN and muscle activity with regards to the same joint in other preparations (Johnston and Levine 2002; Knebel et al. 2017; Ryckebusch and Laurent 1994).

To record depressor MN activity, extracellular hook electrodes (Schmitz et al. 1988) were placed on the lateral nerve C2 of the *nervus cruris* (Graham 1985), which carries the axons that innervate the depressor trochanteris muscle (Bässler and Wegner 1983; Goldammer et al. 2012). Signals were preamplified by an isolated low-noise preamplifier (100-fold; model PA101; Electronics workshop, Zoological Institute, University of Cologne). The signal was further amplified 10-fold and high- and low-pass filtered (high pass: 200 Hz, low pass: 3 kHz) using a standard four-channel amplifier/signal conditioner (model MA102, Electronics workshop, Zoological Institute, University of Cologne). The signal was digitized and recorded at a sampling rate of 12 kHz, using the Micro 1401-3 analog-to-digital converter (Cambridge Electronic Design, Cambridge, UK) and Spike2 software (Cambridge Electronic Design).

Intracellular recordings were performed according to established procedures (Büschges 1998) in bridge mode (intracellular amplifier SEC-10L, NPI Electronic, Tamm, Germany) using electrodes with resistances ranging from 15 to 35 MΩ. Glass microfilaments were pulled using a Sutter Micropuller (P-1000, Sutter Instruments, Novato, CA) and filled with 3 M KAc/0.1 M KCl or 5% neurobiotin in 3 M KAc/0.1 M KCl.

Data Analysis

Phase analysis of rhythmic activity in the meso- and metathoracic ganglia. To investigate potential interactions between meso- and metathoracic CPGs that drive the trochanteral MN pools in the absence of sensory input, we chose and adapted time series analysis methods widely used in electrodiagnostic medicine and functional neuroimaging techniques to suit our requirements for analyzing nonstationary extracellularly recorded rhythmic motor activity (Kralemann et al. 2008; Pikovsky et al. 2001; Tass et al. 1998).

A representative recording of contralateral depressor nerve activity in the isolated mesothoracic ganglion after application of 5 mM

pilocarpine serves to demonstrate the method used (Fig. 1*A*). First, we removed direct current offset and then rectified and smoothed each extracellular waveform signal with a time constant of 0.05 s (Fig. 1*B1*). Then waveforms were resampled to a rate of 100 Hz, and data were extracted as a time series. The real data sequence was then transformed to a discrete-time analytic signal according to the formula $x = xr + i \times xi$ (xr is the real part corresponding to the original data, and xi is the imaginary part containing the Hilbert transform). The resulting signal (Fig. 1*C1*) has the same amplitude and frequency content as the original sequence and includes phase information that depends on the phase of the original data. The Poincaré section (Fig. 1*C1*, shaded horizontal line) was used to mark cycle onsets and

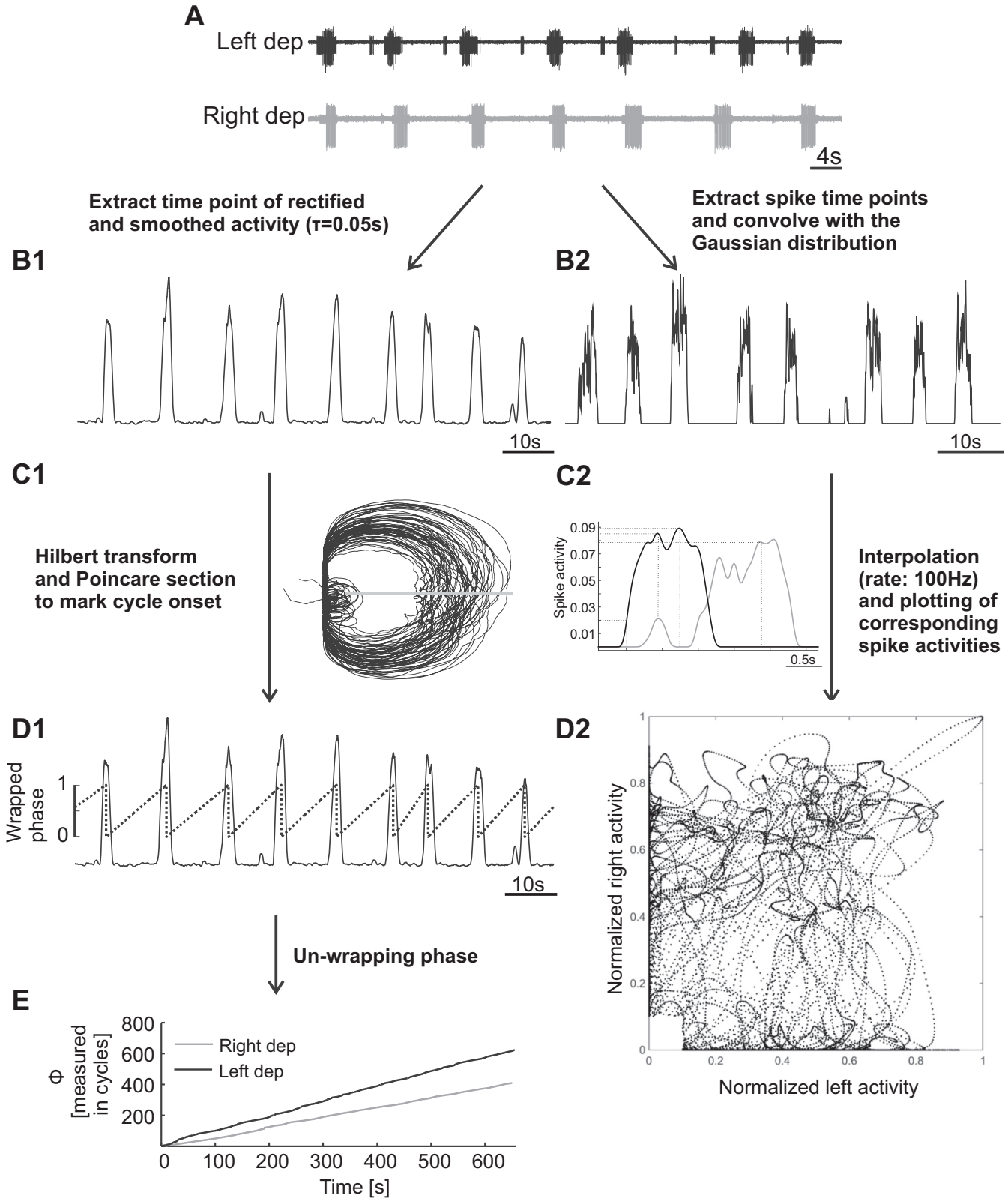

determine the instantaneous, wrapped phase, increasing from 0 to 1 for each cycle (Fig. 1*D1*). Finally, we unwrapped the phase and let it continuously grow from one cycle to the next (cumulative phase), and we plotted this infinite phase over the recording time (Fig. 1*E*, shaded curve). In parallel, all of the above steps were applied for the contralateral nerve recording, and its infinite phase development was also plotted (Fig. 1*E*, solid curve). Subtracting the two curves yields the phase difference of the two rhythms (see Fig. 2*B2*). Furthermore, we calculated the phase difference between the two rhythmic signals and plotted the angle distribution on the unit circle. For this, the rhythmic activity that had more cycles was used as a reference, and the relative phase of the cycle onset of the contralateral nerve rhythm was calculated throughout the recording. The angles extracted were binned, and the number of events in each bin was normalized to the sum of the events. We also calculated the percentage of the cycles showing a phase difference within the interval $0 \pm 45°$ or $180 \pm 45°$, as an indicator of the tendency for in- and antiphase activity, respectively.

Synchronization analysis of contralateral rhythmic motor activity in the prothoracic ganglion. In the isolated prothoracic ganglion, pilocarpine-induced motor activity was more variable than in the two other thoracic ganglia. It often consisted of periods of regular bursting in both depressor MNs (i.e., the SDTr and the FDTr). These periods intermingled with intervals of long SDTr bursts. The discrete analytic signal did not show clear loops. Consequently, the Poincaré section often resulted in errors such as double cycle onsets, rendering the determination of cycle onset unreliable. Thus the aforementioned phase analysis method could not be applied.

To investigate synchronization between contralateral networks in the prothoracic ganglion, we followed a different approach. We first marked all spike events in the recordings and extracted the corresponding time series at a sample rate of 1,000 Hz. Then data were smoothed by convolving the spike time series with a Gaussian function (Fig. 1*B2*). Lastly, we resampled both resultant time series to 100 Hz (Fig. 1*C2*) and plotted the normalized activity of each data trace against the other (Fig. 1*D2*). In case of synchronous activity, spike events will occur at a similar time, and high normalized activity in one recording trace will correspond to high activity in the other (Fig. 1*D2*; data points clustered at the center of the plot). Conversely, out-of-phase events will result in data accumulation along the axes (Fig. 1*D2*, data points close to the *x*- and *y*-axes of the plot). Completely random data corresponding to uncoordinated nerve activity are expected to cluster around the origin. Lastly, we binned our data in a 15×15 grid and generated two-dimensional probability distributions (see Figs. 6 and 7 in RESULTS). To increase contrast, we excluded from the analysis all data that correspond to single or double spikes with normalized activity up to 0.1 and result from noise in the nervous system. For the same reason, the map scale was adjusted and applies to all figures (it is therefore shown only once on Fig. 6*B2*).

Statistical Analysis

We used the MATLAB toolbox CircStat (Berens 2009) for statistical analysis of circular data. We calculated the mean phase difference with 95% confidence interval (CI) estimation for the population and the angular deviation from the mean direction. To measure the spread around the mean, we estimated the resultant vector length (r-vector). Circular uniformity was tested using the "omnibus test" (circ_otest function, CircStat toolbox). Finally, we used a test similar to the one-sample *t*-test on a linear scale (circ_mtest function, CircStat toolbox) to examine whether the mean angle of our data is equal to a specified direction.

RESULTS

Coordination Between Contralateral Depressor Activity in the Isolated Mesothoracic Ganglion

To determine whether depressor MN pools on both sides of the mesothoracic segment are centrally coupled, we analyzed the coordination between rhythmically active depressor MNs ($N = 4$). For this, we recorded depressor MN activity from both sides of the completely isolated and deafferented mesothoracic ganglion following pilocarpine application. We calculated the mean cycle period of each depressor rhythmic activity, and the average mean cycle period of the four preparations was 4.6 ± 1.4 s. As reported previously for MN pools of the thoraco-coxal joint (Büschges et al. 1995), we did not observe systematic cycle-to-cycle coupling between left and right depressor MN activity. However, we detected periods in which bursting activity appeared to be almost synchronous (Fig. 2*A*, solid and shaded traces). To systematically analyze the relationship between rhythmic motor activity on both sides of the mesothoracic ganglion and its development over time, we first plotted the infinite phase of each motor nerve trace individually (Fig. 2*B1*). This phase analysis demonstrated an almost linear phase increase and parallel phase development for both depressor MNs, as indicated by the slopes of the two phase curves. Stable relationships between the frequencies of the two rhythms would be a prerequisite for synchronization. To test whether any frequency locking existed, we then computed the instantaneous frequency of each MN trace. The overall frequency ratio was irregular and fluctuated close to 1, suggesting that the frequencies were similar (data not shown). The activity of the two depressor MN pools retained a nearly constant phase difference with each other, as was also exemplified by the unsteady phase difference curve (Fig. 2*B2*). The above results are indicative of weak coupling between contralateral depressor MNs.

Nevertheless, the overall phase difference distribution, calculated throughout >600 s of recording, showed distinct peaks (Fig. 2*C*, solid line). The data showed statistically significant deviation from circular uniformity ($P < 0.001$). The mean direction was 352° (95% CI: 328 to 15°) with an angular deviation of 64.5° and an r-vector of 0.37. In this recording, about one-half of the cycles (48%) showed a phase difference within the interval of 315 to 45° ($0 \pm 45°$). These values are indicative of synchronized activity and suggest weak in-phase

Fig. 1. Two methods for the analysis of synchronization between contralateral depressor MN activities. *A*: extracellular recording of contralateral mesothoracic C2 nerves innervating the left and right depressor (dep) muscles of the stick insect. Rhythmic activity was induced by application of 5 mM pilocarpine in saline. *B1*: each recording trace (only one is shown here) was rectified and smoothed with a time constant (τ) of 0.05 s. *C1*: each trace was resampled at a rate of 100 Hz and underwent Hilbert transform to automatically mark cycle onsets using the Poincaré section and estimate the wrapped phase. *D1*: wrapped phase defined on the circle from 0 to 1. *E*: infinite (cumulative) phase (Φ) of each nerve. *B2*: time series of spike events were extracted at a sampling rate of 1,000 Hz, and data were smoothed after convolution with the Gaussian distribution (only one trace is shown). *C2*: contralateral spike activity was compared after applying interpolation to introduce corresponding values every 10 ms in both time series. In asynchronous bursting, high-spike activity in one nerve corresponds to low activity in the contralateral nerve. *D2*: plot of the normalized spike activity of each data trace against activity of the other. Synchronous activity results in data points close to the center of the plot. Asynchronous spike events result in data points close to the *x*- and *y*-axes of the plot.

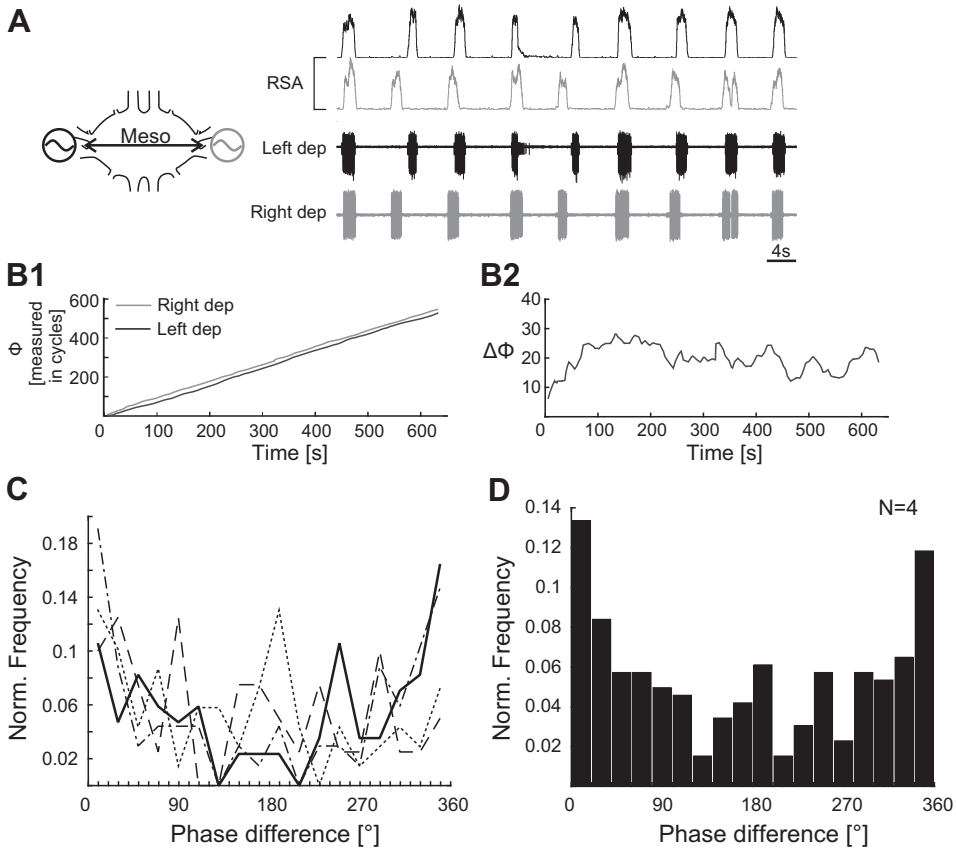

Fig. 2. Phase analysis of the isolated mesothoracic (Meso) ganglion. *A*: extracellular recording of left (solid trace) and right (shaded trace) depressor (dep) MN activity in the isolated Meso ganglion. Rhythmic activity was induced by application of 5 mM pilocarpine in saline. Rectified and smoothed activity (RSA) allows direct comparison. *B1*: the infinite phase (Φ) of each nerve is plotted throughout the recording. Activity of contralateral MNs is not systematically coupled. *B2*: phase difference (ΔΦ) time course throughout the recording. *C*: overall ΔΦ distributions for four different animal preparations plotted on top of each other. They show a tendency for in-phase activity. The solid line corresponds to the preparation analyzed in previous subfigures. *D*: normalized and pooled data from four different animal preparations show a clear peak at the start of the cycle. *N*, no. of animal preparations.

coupling between the underlying networks driving the depressor MNs on either side of the mesothoracic ganglion. Results obtained from three further preparations were consistent with these observations, showing distinct peaks around 0° (Fig. 2*C*, dashed lines). The statistical hypothesis for mean direction toward 0° could not be rejected in any preparation, implying that all distributions showed mean angles equal to 0°. The phase difference distribution after pooling the data from all four animals, corresponding to a total recording time of ~2,400 s, showed a preferred direction ($P < 0.001$) with a mean angle of 5° (95% CI: 347 to 22°) and a 69° angular deviation (Fig. 2*D*). The r-vector length was 0.28. However, only 44% of the cycles showed phase relationships of $0 \pm 45°$, indicating that interactions between contralateral networks driving the depressor MNs are weak and allow for other phase relationships to develop as well (i.e., peaks at various angles in phase distributions). Taken together, these observations suggest that the CPGs generating rhythmic activity in depressor MNs on the left and right side of the isolated and deafferented mesothoracic ganglion are weakly coupled and show a tendency for in-phase relationship with each other.

Coordination Between Contralateral Depressor MN Activity in the Isolated Metathoracic Ganglion

Next, we applied the same approach to analyze the phase relationships between contralateral rhythmically active depressor MNs in the isolated metathoracic ganglion ($N = 4$). The mean of the mean cycle periods was 4.9 ± 1.37 s. Similar to the situation in the mesothoracic ganglion, we did not observe systematic cycle-to-cycle coupling between rhythmic activity in depressor MNs on either side of the metathoracic ganglion. However, unlike the isolated mesothoracic ganglion preparation, contralateral depressor MN bursts in the isolated metathoracic ganglion were found to be antiphase for many cycles (Fig. 3*A*). Infinite phases of the two rhythmically active metathoracic depressor MN pools also developed linearly (Fig. 3*B1*). The corresponding phase curves had different slopes, indicating different phase development for each of the two MN rhythms. Although variable, their frequency ratio fluctuated around 1. This indicated similar, but not systematically coupled, frequencies (data not shown). Moreover, the phase difference between left and right depressor rhythms continuously shifted throughout the recording, showing only few and short intervals during which the two rhythms nearly retained a constant phase relationship (Fig. 3*B2*). This suggests that there is no strong and systematic coupling between the two sides. The phase distribution calculated for a 615-s recording period (Fig. 3*C*, solid line) highlighted a slight tendency for antiphase activity with a mean angle of 165° (95% CI: 138 to 192°), angular deviation of 66°, and r-vector length of 0.34. Here, 43% of the cycles had a phase difference of $180 \pm 45°$. This distribution was the only one of the four that significantly deviated from the uniform distribution ($P < 0.001$). However, two other preparations also showed a tendency for out-of-phase activity between contralateral depressors (Fig. 3*C*, solid and dash-dotted lines). For all distributions, the statistical hypothesis for mean direction toward 180° could not be rejected. A clear phase preference close to the start of the cycle was observed in one preparation (Fig. 3*C*). Pooled data (~2,500 s of total recording time) resulted in a more uniform phase difference distribution than that of the isolated mesothoracic ganglion, as indicated by the higher P value ($0.001 < P < 0.01$),

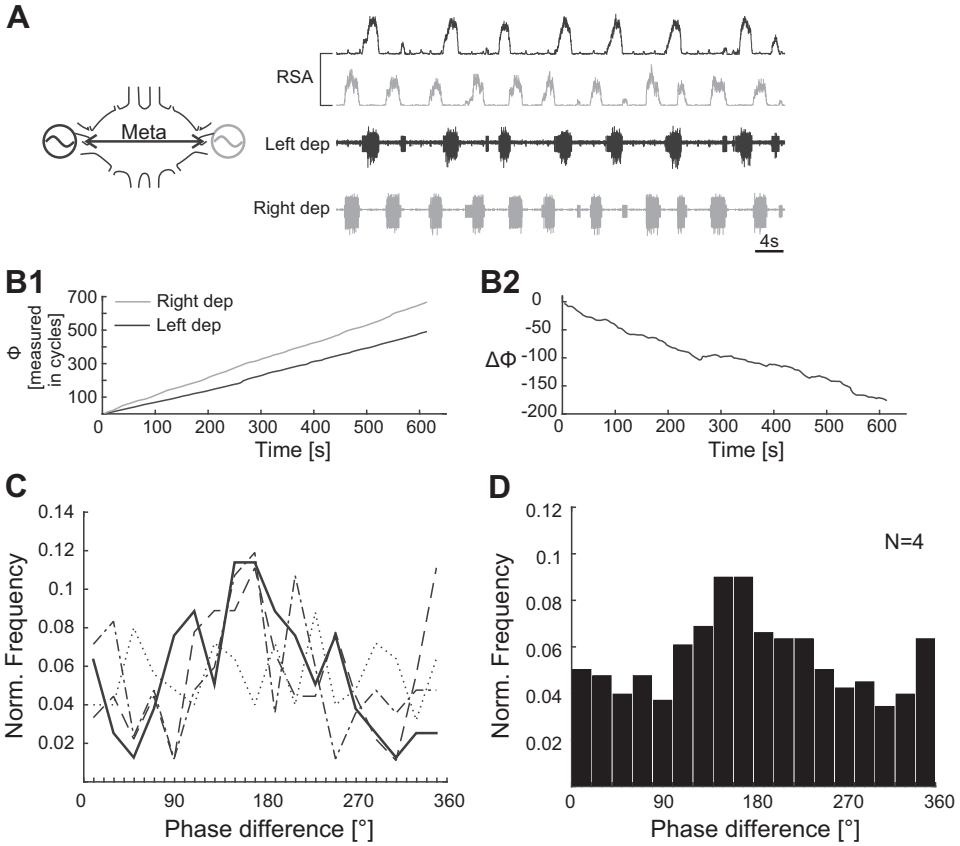

Fig. 3. Phase analysis of the isolated metathoracic (Meta) ganglion. *A*: extracellular recording of left (solid trace) and right (shaded trace) depressor (dep) MN activity in the isolated Meta ganglion. Rhythmic activity was induced by application of 5 mM pilocarpine in saline. Rectified and smoothed activity (RSA) allows direct comparison. *B1*: the infinite phase (Φ) of each nerve is plotted throughout the recording. Activity of contralateral MNs is not systematically coupled. *B2*: phase difference (ΔΦ) time course throughout the recording. *C*: overall ΔΦ distributions for four different animal preparations plotted on top of each other. They show a tendency for out-of-phase activity. The solid line corresponds to the preparation analyzed in previous subfigures. *D*: normalized and pooled data from four different animal preparations shows a smooth peak at around 180°. *N*, no. of animal preparations.

with a mean direction of 166° (95% CI: 137.5 to 195°), 75° deviation, and an r-vector of 0.15 (Fig. 3*D*). Only 33% of the cycles of the pooled data showed clear antiphase activity, with phase differences between 135 and 225° (180 ± 45°).

Thus consistent with our results from the mesothoracic ganglion, weak coupling exists between rhythmic depressor MN activity on both sides of the isolated and deafferented metathoracic ganglion. However, phase relationships vary between preparations and do not consistently show a distinct direction, although a slight tendency for antiphase activity is present.

Intrasegmental Coordination of Depressor Activity Is Influenced by Intersegmental Signals

Next, we studied the influence of potential intersegmental signaling on left-right coordination in the meso- and metathoracic ganglia. To do this, we extracellularly recorded pilocarpine-induced activity in contralateral depressor MNs of the interconnected meso- and metathoracic ganglia, and we analyzed the phase relationships between contralateral CPG outputs. Interestingly, we observed a striking change in rhythmic activity in both ganglia, namely synchronous, in-phase bursting activity of all depressors for many consecutive cycles (Fig. 4*A*). This change is best exemplified by comparing Figs. 3*A* and 4*A*. Although these intervals of simultaneous bursting were often interrupted by gaps in activity or double bursts, coordination recovered within a few cycles (see asterisks in Fig. 4*A*). This indicates the existence of an underlying mechanism that induces weak coupling between depressor MNs in the meso- and metathoracic ganglia.

In the mesothoracic ganglion, phase analysis of the observed rhythmicity revealed long intervals during which the frequencies of contralateral CTr-joint CPGs were similar (data not shown). During such intervals, rhythmic activity was coupled and retained a constant phase difference between contralateral sides for >200 s (Fig. 4*B1*). Notably, such long periods of coupled activity have never been detected in isolated ganglia. The same holds for the metathoracic ganglion, although rhythmic activity on both contralateral sides was more variable, and intervals of coupled activity were shorter in duration compared with those of the interconnected mesothoracic ganglion (Fig. 4*B2*). These results suggest that intersegmental signals between both thoracic segments can increase contralateral coupling between depressor MNs in both ganglia and influence contralateral phase relationships.

We also calculated the overall phase difference distribution between contralateral depressor rhythms of both ganglia. All distributions of the mesothoracic ganglion ($N = 7$) and 8/10 metathoracic preparations significantly deviated from the null hypothesis of uniformity at the 95% level at least. They all showed clear peaks at or close to 0° (Fig. 4, *C1* and *C2*). Contralateral depressor rhythms in the interconnected mesothoracic ganglion recording shown in Fig. 4 had a mean phase difference of 0° (95% CI: 353 to 8°), an angular deviation of 34°, and an r-vector length of 0.83. Contralateral depressor rhythms in the interconnected metathoracic ganglion had a mean phase difference of 23° (95% CI: 7.5 to 39°), with a deviation of 61° and an r-vector length of 0.44. Pooled data extracted from 3,588 s of recording time showed that contralateral depressor MNs of the mesothoracic ganglion were strictly

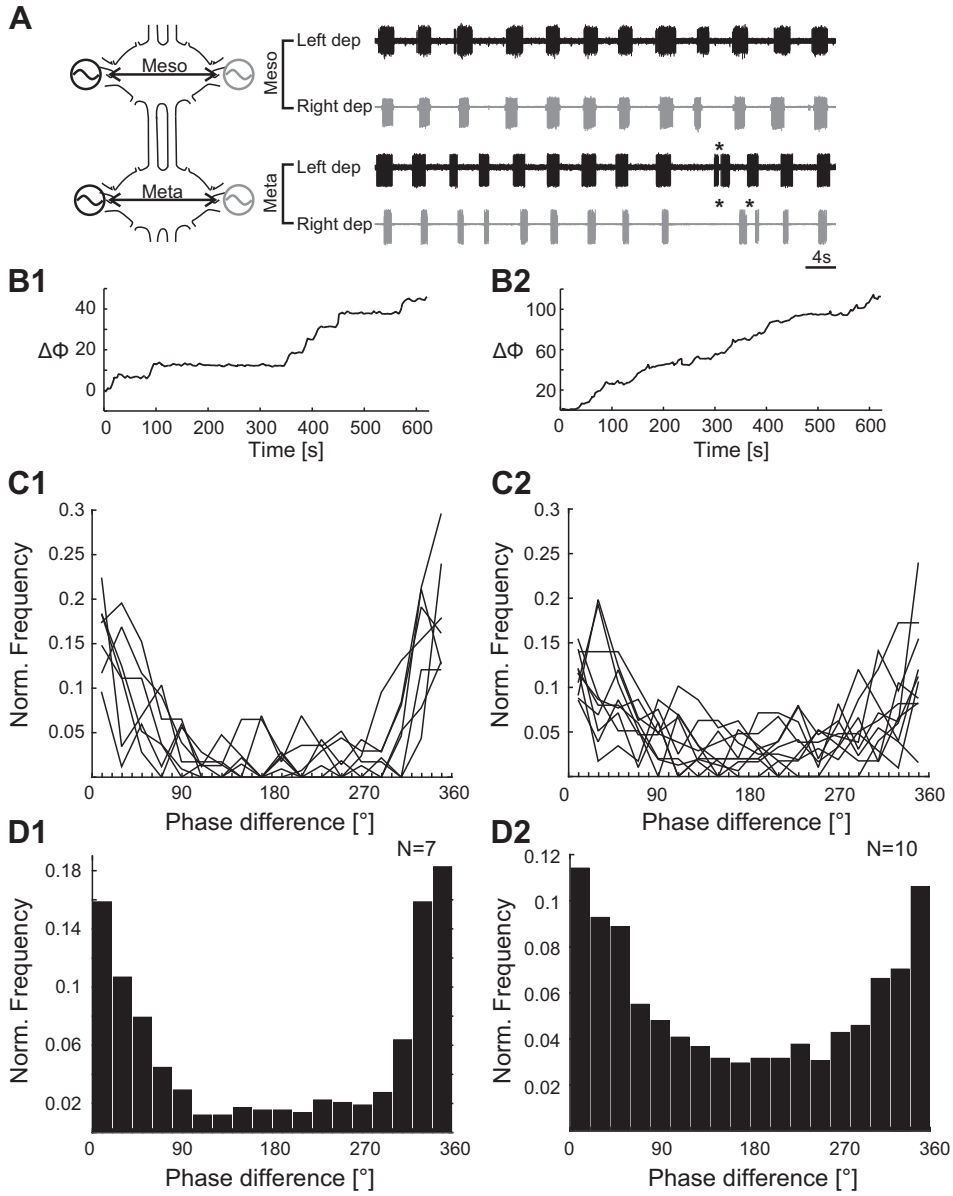

Fig. 4. Phase analysis of the interconnected meso- (Meso) and metathoracic (Meta) ganglia. *A*: extracellular recording of contralateral depressor (dep) MN activity in the interconnected Meso and Meta ganglia. Rhythmic activity was induced by application of 5 mM pilocarpine in saline. Simultaneous bursting activity of contralateral depressor MNs is observed in both ganglia. Approximately simultaneous bursting was often interrupted by gaps in activity or double bursts (asterisks). *B1*: the phase difference (ΔΦ) between contralateral rhythmic activity of the interconnected Meso ganglion shows very long recording intervals of coupled activity. *B2*: the ΔΦ between contralateral rhythmic activity of the interconnected Meta ganglion fluctuate more, but also show long intervals of coupled activity. *C1* and *C2*: overall ΔΦ distributions between contralateral activity of the interconnected Meso (*C1*) and Meta ganglion (*C2*) plotted on top of each other. All distributions in both ganglia (7 in *C1* and 10 in *C2*) show clear peaks at the start of the cycle. Intersegmental connection has an influence on contralateral coupling. *D1* and *D2*: distributions based on normalized and pooled data from 7 and 10 different animal preparations for the interconnected Meso (*D1*) and Meta ganglion (*D2*). There is a preference for in-phase activity between contralateral depressor motor outputs of both interconnected ganglia. *N*, no. of animal preparations.

in-phase with a mean angle of 360° (95% CI: 354.5 to 4.5°), an angular deviation of 52°, and an r-vector length of 0.59 (Fig. 4*D1*). More than one-half of the cycles (66%) had a phase difference of 0 ± 45°, while the rest of the cycles showed phase differences distributed all around the unit circle. Pooled data from the interconnected metathoracic ganglion showed a mean angle of 10° (95% CI: 2 to 18°), an angular deviation of 67.4°, and an r-vector length of 0.31. Here, 43% of the cycles showed phase differences within the interval of 0 ± 45°.

Apparently, neural signals transmitted through the connectives that link the two ganglia stabilize contralateral phase relationships and/or restrict them to certain values. Moreover, intersegmental signals coming from the mesothoracic ganglion have a significant influence on coordination between rhythmic activity of contralateral depressor MNs in the metathoracic ganglion, leading to long intervals of in-phase activity (compare Figs. 3*B2* and 4*B2*). To substantiate this observation, we split the bath between the meso- and the metathoracic ganglia and applied pilocarpine first to the metathoracic ganglion and, subsequently, to both ganglia ($N = 6$).

After activation of the metathoracic ganglion, the overall distributions of phase differences in six different preparations showed peaks at different angles throughout the cycle (Fig. 5*B1*). In two preparations, peaks were formed either at 180°, or between 0 and 90° and close to 270°, while distributions of all other preparations did not show such peaks. Interestingly, after subsequent activation of rhythmic activity in the mesothoracic ganglion, a tendency toward in-phase activity was apparent in four out of six preparations (Fig. 5*B2*). The phase distributions corresponding to these preparations showed a significant directedness toward 0°, whereas the hypothesis for mean direction toward 180° was rejected. Pooled data from 3,200 s of recording showed a uniform distribution ($P = 0.954$) and no distinct phase difference preference for contralateral metathoracic activity before activation of rhythmic activity in the mesothoracic ganglion, as indicated by a low r-vector length (0.01; Fig. 5*C1*). Following application of pilocarpine to the

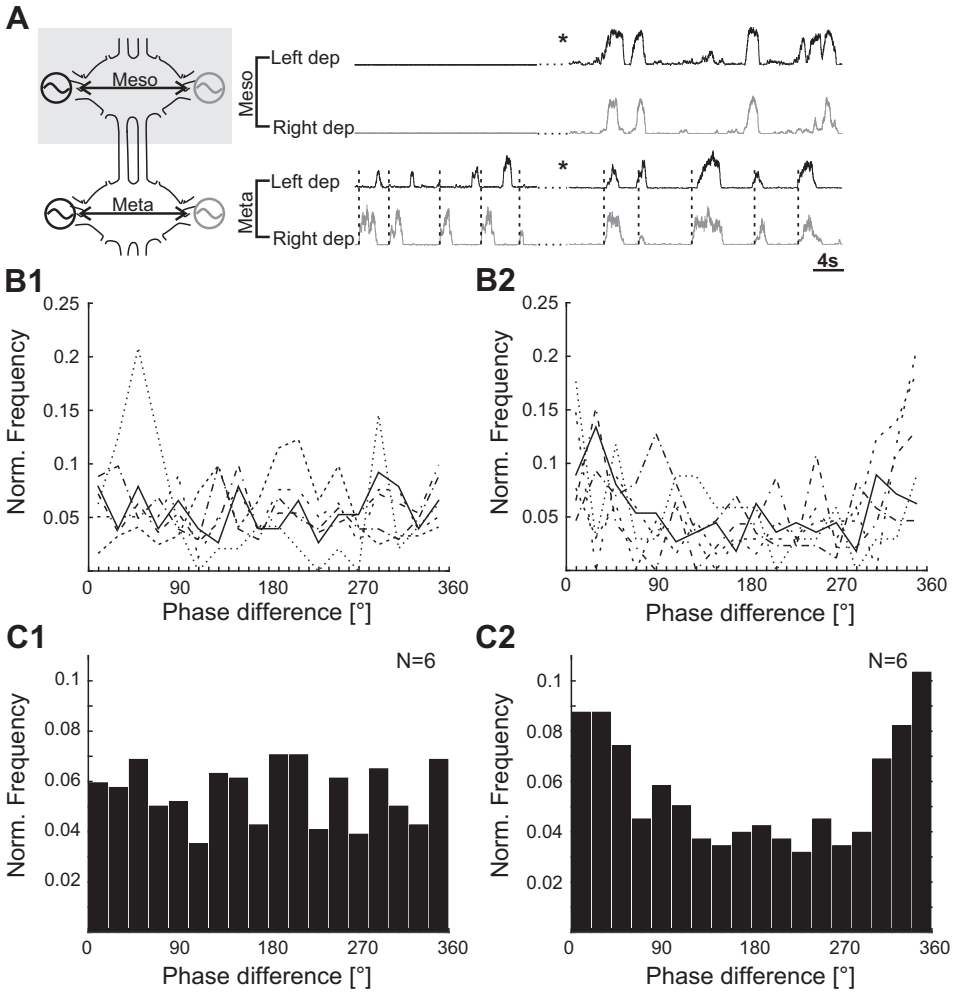

Fig. 5. Phase analysis of the interconnected metathoracic (Meta) ganglion before and after activation of the mesothoracic (Meso) networks. *A*: extracellular recording of contralateral depressor (dep) MN activity in the interconnected Meso and Meta ganglia. Rectified and smoothed activity (RSA) is shown to allow direct comparison. Bath was split with a silicone wall between the two ganglia. Rhythmic activity was induced by application of 5 mM pilocarpine, first on the Meta (left part of the recording) and subsequently on the Meso ganglion (right part). *B1*: overall phase difference ($\Delta\Phi$) distributions between contralateral activity of the interconnected Meta ganglion before pilocarpine application on the Meso ganglion. Distributions show no clear preference for any certain $\Delta\Phi$. *B2*: overall $\Delta\Phi$ distributions between contralateral activity of the interconnected Meta ganglion after pilocarpine application on the Meso ganglion. Intersegmental connection has an influence on contralateral coupling. *C1* and *C2*: distributions of the $\Delta\Phi$ between contralateral depressor MNs of the interconnected Meta ganglion, based on normalized and pooled data from six different split-bath preparations, before (*C1*) and after (*C2*) application of pilocarpine on the Meso ganglion. Distribution is uniform before (*C1*), whereas it shows a preference for in-phase activity after activation of Meso networks (*C2*). *N*, no. of animal preparations.

mesothoracic ganglion, the distribution of pooled data (2,600 s) formed a clear peak ($P < 0.001$) around the beginning of the cycle. These data showed a mean angle of 10° (95% CI: 352 to 27°), and the r-vector length was as high as 0.24, indicating higher tendency for in-phase activity (Fig. 5*C2*). Before the activation of the mesothoracic networks, only 26% of the cycles in the interconnected metathoracic ganglion had phase differences in the range of $0 \pm 45°$, whereas this percentage was increased to 38% thereafter. These experiments support our previous conclusion that intersegmental neural signals operating between the two thoracic ganglia induce weak in-phase coupling of rhythmic activity in depressor MNs of both segments.

Coordination Between Contralateral Depressor MNs in the Isolated and Interconnected Prothoracic Ganglion

We first investigated coupling between contralateral depressor MNs in the isolated prothoracic ganglion. Here, the mean of the mean cycle periods of six different preparations was 1.79 ± 0.24 s. This is almost three times shorter than the mean cycle periods of the isolated meso- and metathoracic ganglia. In prothoracic recordings, intervals of activated bursts consisting of both the SDTr and FDTr units alternated with long SDTr bursts, and we observed no clear coordination pattern between contralateral sides (Fig. 6*A*). Indeed, recurrent patterns of synchronous bursting were detected in one preparation only, which implied weak interaction between the networks that drive contralateral depressors of the prothorax (data not shown). Plotting spike activity of each depressor MN against its contralateral counterpart confirmed the above observations. Data were randomly distributed and did not show clear clusters (Fig. 6, *B1* and *B2*). Collectively, in five out of six preparations, we found no obvious coordination patterns between the contralateral sides, as pooled data of all preparations (3,900 s) showed no distinct pattern of activity (Fig. 6, *C1* and *C2*). Data in these two plots built up around zero, indicating a random distribution. Thus there exists no clear coordination between contralateral CTr-joint CPGs in the isolated prothoracic ganglion.

We next investigated whether intersegmental signals from the mesothoracic segment would affect left-right coordination of CTr-CPGs in the prothoracic ganglion. For this, we recorded contralateral depressor activity in the prothoracic ganglion, while it was connected to the mesothoracic ganglion after pilocarpine application to both ganglia (Fig. 7*A*). A comparison of the depressor MN activity of both ganglia showed no systematic coupling, although synchronous bursting intervals in both traces were intermingled with periods during which only slow depressor units were active. However, plotting the corresponding normalized activity of the two contralateral depressor MN pools of the prothoracic ganglion against each other revealed not only data points close to the two axes, but

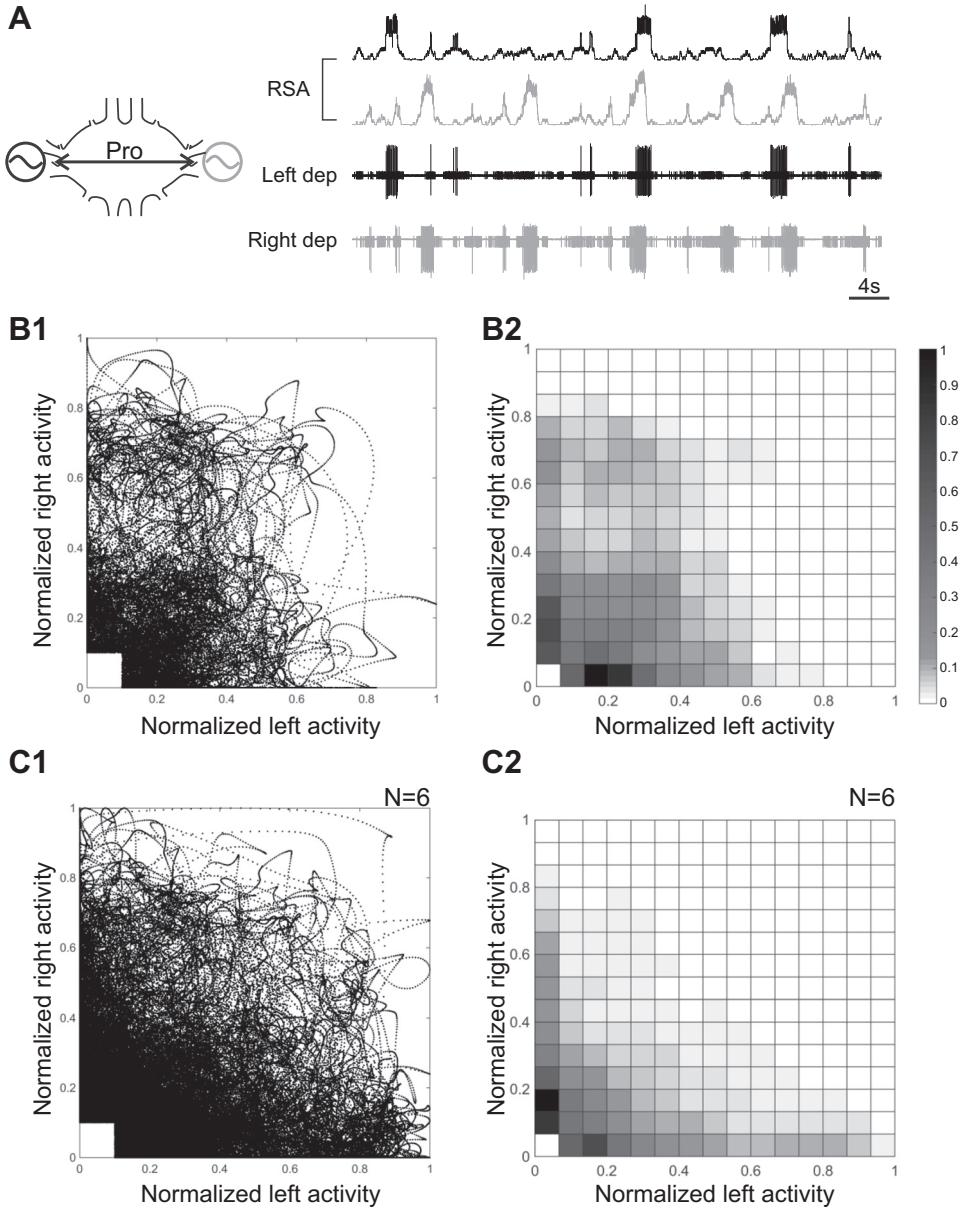

Fig. 6. Synchronization analysis of the isolated prothoracic (Pro) ganglion. *A*: extracellular recording of contralateral depressor (dep) MN activity in the isolated Pro ganglion. Rhythmic activity was induced by application of 5–7 mM pilocarpine in saline. RSA, rectified and smoothed activity. *B1*: spike activity of each nerve was smoothed, and corresponding spike activity values at a rate of 100 Hz throughout the recording were plotted against each other after being normalized to the maximum activity value. The plot shows a random distribution of data, indicating no clear coordination pattern between contralateral depressor MNs. *B2*: heat map based on the data shown in *B1*. *C1*: pooled data from six preparations. Data are randomly distributed, and thus MNs show no clear coordination. *C2*: heat map based on data shown in *C1*. *N*, no. of animal preparations.

also a higher frequency of data points in the center of the plot at similar levels (around 0.6) of normalized activity (Fig. 7, *B1* and *B2*). This clustering of data indicated a higher likelihood for synchronous spiking between the two depressor MN pools, implying that there is an intersegmental influence on contralateral coordination in the prothoracic ganglion. The same was true, when both caudal ganglia were connected to the prothoracic ganglion (data not shown). Similar synchronous activity was observed between contralateral depressor MNs of the mesothoracic ganglion, while being interconnected to the prothoracic ganglion (data not shown). Distinction between synchronous and asynchronous activity was still evident after pooling the data from all five preparations with a total recording length of ~3,400 s (Fig. 7*C1*). Comparison between the heat map in Fig. 7*C2* with the isolated ganglion (Fig. 6*C2*) clearly shows a lack of coordination in the isolated prothoracic ganglion and how activity was shaped and coordinated when it was interconnected. These results suggest that coordination between contralateral depressor MN pools in the prothoracic ganglion is influenced by intersegmental signals from the mesothoracic ganglion, resulting in synchronization and coordination between contralateral prothoracic CTr-CPGs.

Influence of Contralateral Mesothoracic Depressor CPG Activity on Contralateral Depressor MNs

Having identified that CTr-joint CPG motor outputs are weakly coupled, we sought to investigate whether ipsilateral depressor MN activity is directly affected by input coming from the contralateral CPG, resulting in weak contralateral coupling. To do this, we tested the effect of MN activity from each side of the ganglion on MN activity in the contralateral side. We combined extracellular recordings of contralateral depressor MN activity with intracellular recordings from either the SDTr or the FDTr located on the right hemisegment of the isolated and deafferented mesothoracic ganglion. In six out of

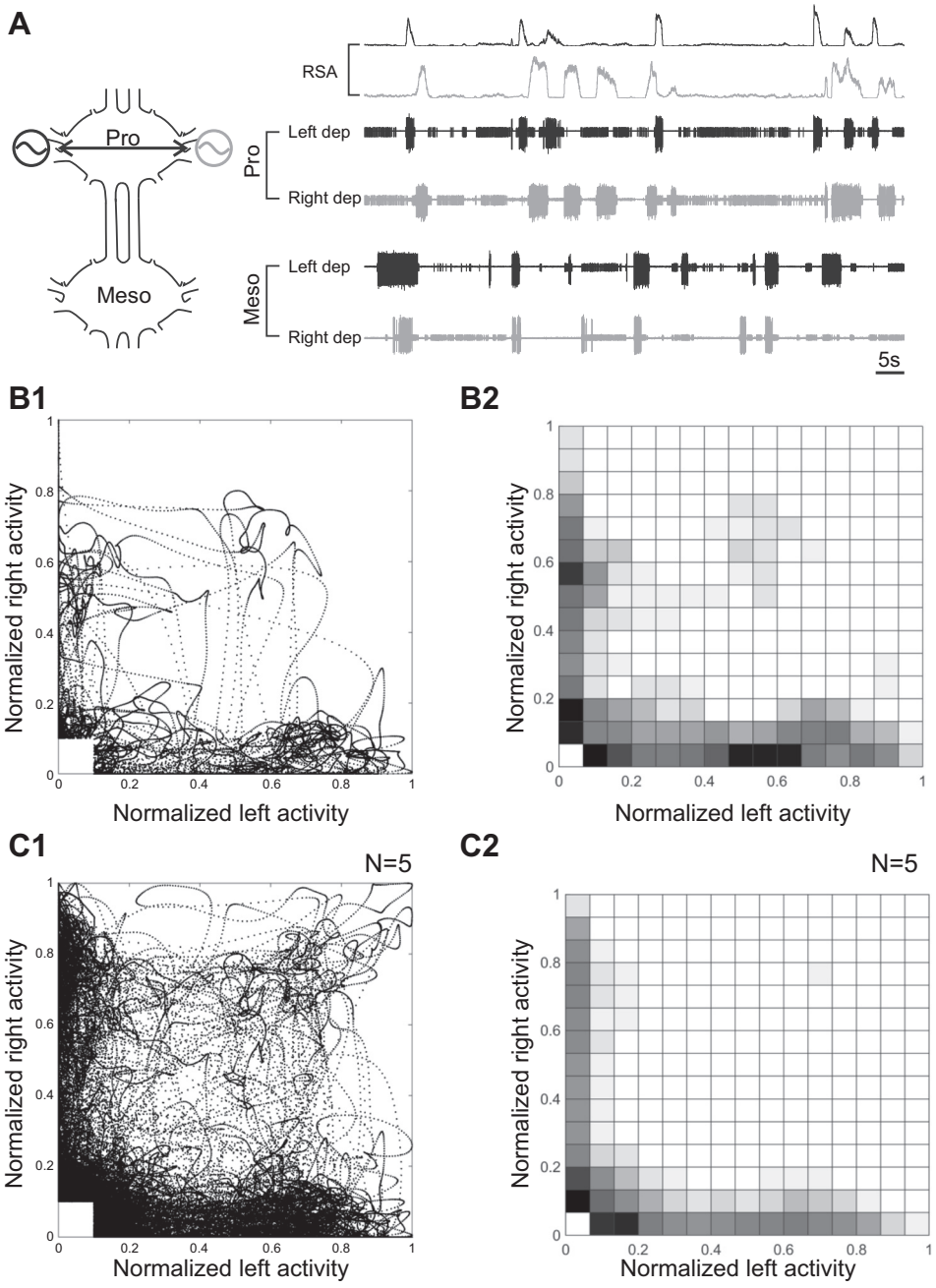

Fig. 7. Synchronization analysis of the interconnected prothoracic (Pro) ganglion. *A*: extracellular recording of contralateral depressor (dep) MN activity in the interconnected Pro and mesothoracic (Meso) ganglia. Rhythmic activity was induced by application of 5–7 mM pilocarpine in saline. RSA, rectified and smoothed activity of the left and right Pro depressor traces. Bursting intervals alternate with long slow unit activation periods. *B1*: normalized spike activity of one Pro depressor is plotted against the contralateral depressor activity. There are clear clusters of data points at around 0.6 close to the two axes (asynchronous activity) and at the center (synchronous activity) of the plot. *B2*: heat map based on the data shown in *B1*. Distinct data clusters indicate coordination of activity between the two MNs. *C1*: pooled data from five preparations. Data are clustered, indicating improved coordination between contralateral depressor MNs when Pro and Meso ganglia are connected. *C2*: heat map based on data shown in *C1*. *N*, no. of animal preparations.

six recordings, we detected no effect on the intracellular trace at the contralateral depressor cycle onset, indicating that there is no direct influence between contralateral depressor MNs (Fig. 8*A*). Superposition of the intracellular recording trace aligned to the cycle onset of either the contralateral (Fig. 8*Bi*) or the ipsilateral (Fig. 8*Bii*) depressor cycle confirmed that the FDTr receives no input related to the contralateral depressor activity. In agreement with these results, current injection of up to 7 nA in a depressor MN on one side had no influence on the rhythm of the contralateral depressor activity. The input resistance of the neuron showed no alteration correlated with the left depressor cycle (Fig. 8*C*). Therefore, based on activation patterns in the presence of pilocarpine, it is unlikely that there exists a direct influence of the CTr-joint CPG on the contralateral depressor MN.

DISCUSSION

In the present study, we analyzed intra- and intersegmental interactions between segmental CPGs of the depressor trochanteris MNs in all three isolated or interconnected thoracic ganglia of the stick insect. According to our data, there is no strong and persistent cycle-to-cycle coupling between contralateral sides of any of the three thoracic ganglia in the presence of pilocarpine. More particularly, we observed a tendency for certain phase differences in the isolated meso- and metathoracic ganglia (Figs. 2*D* and 3*D*) and no evidence for coordination in the isolated prothoracic ganglion (Fig. 6, *C1* and *C2*). However, when ganglia were connected, intrasegmental CPG coordination was modified, so that the likelihood for coordinated activity increased for all ganglia (Figs. 4, *D1* and *D2*, and 7). Finally, intracellular recordings of depressor

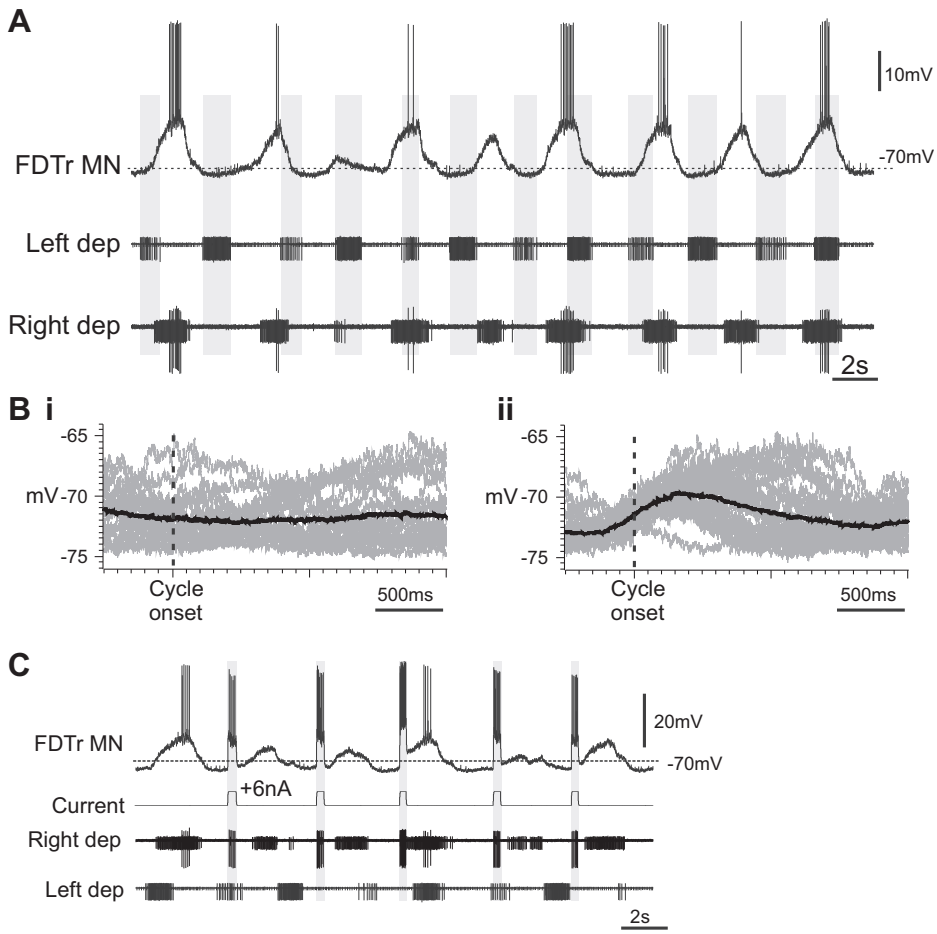

Fig. 8. Intracellular recording of the fast depressor (dep) MN of the isolated mesothoracic ganglion. *A*: intracellular recording of the fast depressor MN (FDTr) from the right hemisegment, combined with extracellular recording of contralateral depressor MN activity in the isolated mesothoracic ganglion. Rhythmic activity was induced by application of 5 mM pilocarpine in saline. There was no FDTr membrane potential modulation in phase with the contralateral depressor burst onset (shaded bars). *B*: superpositions of the intracellular trace aligned according to the contralateral-left (*i*) or the ipsilateral-right (*ii*) depressor cycle onset. For this analysis, an interval was chosen, during which the FDTr was not spiking. No input in phase with the contralateral cycle onset could be observed in the FDTr trace. *C*: rectangular depolarizing current pulses of 6 nA applied on FDTr had no influence on contralateral depressor activity or rhythmicity.

MNs in the isolated mesothoracic ganglion showed no direct interaction between depressor CPG networks and contralateral MNs (Fig. 8). Our study highlights the presence of weak central intersegmental interactions between depressor MNs in the stick insect walking system, giving rise to synchronous segmental activity, a coordination pattern that is not observed in freely walking insects.

Coordination in Isolated Ganglia

We have shown that contralateral depressor rhythms are apparently not coordinated in the isolated prothoracic ganglion, whereas in the meso- and metathoracic ganglia they show a tendency for in-phase and antiphase activity, respectively.

Front, middle, and hind legs are structurally and functionally similar to each other, and they all actively contribute to walking on horizontal surfaces. Nevertheless, front legs have a special role, as they can perform additional steps or searching movements independently from other legs (Cruse 1976; Grabowska et al. 2012). Moreover, front legs in swing may perform retargeting movements that result in leg positioning at the height of the last antennal contact on the substrate (Schütz and Dürr 2011). Lastly, front legs have been shown to play only a minor role in propulsion and body weight support of *C. morosus* (Dallmann et al. 2016). Taken together, our findings suggest that the weak central influences between contralateral prothoracic depressor CPGs reported here make those networks more susceptible to sensory and descending input and add to the observed flexibility and autonomy of the front legs. This conclusion agrees with behavioral data that show stronger coordination between the two front legs compared with all other legs in preparations that are not deprived of sensory input (Cruse and Saxler 1980; Dean 1989).

Our results suggest that central coupling interactions are more important for contralateral depressor coordination in the meso- and metathoracic ganglia. In accordance with the data of Knebel et al. (2017), we observed a tendency for in-phase depressor MN activity in the isolated mesothoracic ganglion. In freely behaving animals, in-phase depression of contralateral legs can be observed after synchronous elevation of legs in one segment (Cruse and Knauth 1989; Graham 1985; Wendler 1966). In addition, forces generated by two stationary middle legs on the ground oscillate in-phase, while all other legs walk on a slippery surface (Cruse and Saxler 1980). Thus mesothoracic legs can be synchronously active when they are uncoupled from the front and hind legs. Taken together, the central coupling interactions observed in our experiments result in a default in-phase coordination that could support synchronous middle-leg movements when these legs become uncoupled from the rest. Central in-phase coupling can then be modified by local and intersegmental sensory information to generate behaviorally relevant coordination. The importance of sensory input for coordination in the mesothoracic ganglion has been indicated by behavioral experiments after connective transection (Dean 1989) and in animals walking on a slippery surface (Cruse and Knauth 1989). These experiments show impaired and unclear con-

tralateral coordination between the two middle legs compared with the other two pairs of legs.

In line with data from the locust (Knebel at al. 2017), contralateral depressors of the isolated metathoracic ganglion in the stick insect show a tendency for antiphase activity, exactly as is expected from a freely behaving animal. Our findings are complemented by the previous observation that force oscillations of contralateral, standing hind legs are also out of phase when the other legs walk on a slippery surface (Cruse and Saxler 1980). Considering that hind legs are the closest to the center of mass of the animal, and hind leg depressor joint torques are critical for the animal's propulsion (Dallmann et al. 2016), we, therefore, believe that central coupling mechanisms in the isolated metathoracic ganglion are crucial for the animal's survival by being able to produce functional motor output when all other ganglia are decoupled and sensory information is absent.

Differences in intrasegmental coordination among thoracic ganglia may arise from segmental differences in excitability that could be related to differential expression of muscarinic acetylcholine receptors in each ganglion. At present, no data are available on this issue. Thus, under the assumption that there are no such differences in excitability among thoracic ganglia, we may currently conclude that differences in intrasegmental coordination originate in the different intrasegmental connectivities among the central neural networks that drive the CTr-CPGs of the front, middle, and hind legs of *C. morosus*.

Contribution of Central Intersegmental Pathways to Leg Coordination During Walking

The in-phase coordination patterns we observed in this study after activation of interconnected ganglia may, on initial consideration, appear counterintuitive for understanding walking behavior in the stick insect. It is a nonfunctional coordination pattern that does not resemble any of the walking patterns stick insects use. However, based on this in-phase default output of the deafferented system, we can now provide feasible explanations for previously published observations.

Behavioral studies regarding the influence between walking legs in the stick insect have resulted in seven different effects that legs can have on their immediate neighbors (either contralateral or rostral and caudal), known as the Cruse rules (Cruse 1990; Schilling et al. 2013). These rules are sufficient for generating stable and coordinated six-legged locomotion in computational models (Cruse 1990; Dürr et al. 2004; Schilling et al. 2013). According to *rule 5*, an increase in load in one of the legs will prolong the stance phases in other legs, thereby efficiently distributing load among them (Cruse 1990; Dürr et al. 2004). This intersegmental joint activation of MNs is reminiscent of the in-phase bursting episodes we observed in our experiments. Thus we hypothesize that the centrally generated in-phase coordination patterns result from the stochastic activation of sensory-related central pathways. Pilocarpine could potentially activate such pathways, as it binds to metabotropic acetylcholine receptors that are present on sensory terminals (Trimmer 1995).

In a previous study, the influence of one stepping front leg on MN activity in posterior segments was analyzed (Borgmann et al. 2009). This study showed that activity of the ipsilateral middle and hind leg retractor MNs was entrained in phase with the front leg stepping cycle. However, it is not known whether distinct intersegmental sensory pathways mediate this influence or whether sensory signals are transmitted through specific central connections between CPGs. Here, we show that there are indeed central neural pathways capable of supporting intrasegmental in-phase coupling between CPGs. Interestingly, even signals from a quiescent mesothoracic ganglion seem to affect intrasegmental coordination in the metathoracic ganglion, since phase distributions of contralateral activity in the metathoracic segment, when connected to the quiescent mesothoracic ganglion, were uniform, differing from those of the completely isolated metathoracic ganglion that exhibited slight peaks at 180° (cf., Figs. 3 and 5). Thus, although we cannot exclude the existence of distinct sensory pathways, it is possible that pilocarpine activates sensory afferents that transmit their signals through central connections between CPGs and synchronize CPG activity. If this is true, then we provide further evidence for the hypothesis advanced by Borgmann et al. (2009), according to which an unloaded leg moves in synchrony with its neighboring leg until it receives load information that overrides this weak coordinating influence.

Comparison with Other Insect Walking Systems

Pilocarpine-induced fictive motor patterns in deafferented preparations of the cockroach, hawk moth, locust, and stick insect have been routinely analyzed to detect central interactions between CPGs (Büschges et al. 1995; David et al. 2016; Johnston and Levine 2002; Knebel et al. 2017; Ryckebusch and Laurent 1994). In some preparations, centrally generated coordination patterns were similar to those observed in freely behaving animals, whereas, in others, they substantially differed. This may be due to the relative contribution of central CPG coupling mechanisms for coordination. In addition, behavioral studies have provided input for our understanding of the influence sensory deprivation has on coordination and its dependence on walking speed (Berendes et al. 2016).

Pilocarpine application to the isolated and deafferented thoracic nerve cord of cockroaches results in generation of a tripod-like coordination pattern, similar to the pattern these insects show during actual walking (Fuchs et al. 2011). In a recent study, intersegmental phase relationships between depressor MNs were found to be in accordance with those observed in the walking cockroach (David et al. 2016). Moreover, in the isolated thoracic nerve cord of the hawk moth, pilocarpine elicited strictly alternating activity between contralateral depressor MNs in all segments, and intersegmental coordination resembled a tripod pattern (Johnston and Levine 2002). In contrast, depressor activity in all segments of the locust (Knebel et al. 2017) and the stick insect (in the present study) were found to be weakly coupled in phase, resulting in coordination patterns that have never been observed in behavioral experiments. This reveals that the contribution of central coupling mechanisms to CPG coordination differs among these insect species. Considering that cockroaches and moths show relatively short cycle periods during walking (Couzin-Fuchs et al. 2015; Johnston and Levine 1996) compared with locusts and stick insects (Burns 1973; Graham 1985), our current results support the notion that coordination in slow-walking insects is largely based on sensory input contributions, while

present evidence suggests that, in fast-walking insects, central CPG coupling plays an important role (Couzin-Fuchs et al. 2015; Fuchs et al. 2011). Thus it may be that central CPG connections in the stick insect provide the substrate on which sensory signals can act to shape the coordination pattern into a behaviorally relevant one (Borgmann et al. 2009). In addition, such a hypothesis would explain the entrainment of a leg stump and the subsequent increase in coordination strength observed at fast walking speeds in the fruit fly (Berendes et al. 2016) and the rapid recovery from perturbations during running in cockroaches (Couzin-Fuchs et al. 2015).

A recent study by Knebel et al. (2017) is particularly relevant to our results. In both their study and the present study, the three isolated thoracic ganglia showed different inherent contralateral phase relationships, and, interestingly, depressor MN pools of the isolated metathoracic ganglion showed a high tendency for antiphase activity. Furthermore, intersegmental coupling influenced contralateral phase relationships, especially in the metathoracic ganglion, and, similar to the data we present herein, depressor CPGs of all segments were synchronously active after pilocarpine application to the whole nerve cord. However, data from the present study point out the irregularity of pilocarpine-induced rhythmicity, as there was no consistent cycle-to-cycle coupling. Phase relationships were distributed all around the unit circle, and we only found tendencies for certain phase relationships. Moreover, in contrast to the study by Knebel et al. (2017), pharmacological activation of one ganglion in the present study never induced activity in neighboring, untreated ganglia (Ludwar et al. 2005). Therefore, we conclude that coupling interactions between CPGs in the stick insect are weak, and the deafferented system is characterized by the absence of strict cycle-to-cycle coupling. Given the important roles of local sensory feedback in the generation of stepping (Büschges et al. 2008) and in the coordination between neighboring legs (Borgmann et al. 2009), we propose that sensory signals from the legs serve as a primary source of neural information for generating functional intersegmental leg coordination patterns.

Neural Mechanisms Underlying Intrasegmental CPG Coordination

In vertebrates, there is detailed information on the neural mechanisms underlying intrasegmental coordination. In the mouse spinal cord, flexor extensor CPG activity can be independently induced in each hemisegment, showing that contralateral networks do not form a half-center (Hägglund et al. 2013). Left-right alternation in mice is not only achieved by direct and indirect contralateral MN inhibition via inhibitory and excitatory commissural interneurons, respectively (Butt and Kiehn 2003; Quinlan and Kiehn 2007), but also by excitatory neurons recruited at higher fictive locomotion frequencies (Talpalar et al. 2013). In the lamprey, although there are both excitatory and inhibitory commissural neurons (Biró et al. 2008), contralateral alternating activity is based on glycinergic inhibitory commissural neurons, and hemisegments become synchronously active when glycinergic transmission is blocked (Grillner 2003).

Presumably the simplest CPG organization is the one underlying swimming in the sea slug *Dendronotus iris* (Sakurai and Katz 2016). This CPG consists of only two types of interneurons in each hemisegment that mutually inhibit their contralateral counterparts. Interestingly, the one interneuron type forms an excitatory and an electrical synapse with the contralateral heterologous interneuron, resulting in a twisted half-center CPG organization. In contrast, in the locust wingbeat system, hemisegmental networks in the mesothoracic ganglion are more independent, and rhythm generation in flight MNs appears not to exclusively depend on commissural pathways (Wolf et al. 1988). Moreover, deafferentation has almost no influence on contralateral coordination in this system. Thus coordination between autonomous local hemisegmental networks in the locust flight system is based on a central distributed network (Wolf et al. 1988). In the deafferented preparation of the stick insect, a cut along the midline of the meso- and metathoracic ganglia did not abolish pilocarpine-induced rhythmicity of the protractor and retractor MN pools (Büschges et al. 1995). Considering the intrasegmental influences observed regarding contralateral coordination in our experiments, we hypothesize that such a distributed coordinating network also applies to the stick insect system.

Information regarding intrasegmental coupling between contralateral networks in the stick insect is highly elusive. Here, intracellular recordings of depressor MNs on one side of the ganglion, combined with extracellular depressor MN recordings after pilocarpine application, showed that contralateral depressor MNs are directly connected neither with each other, nor with the contralateral CPG networks. Therefore, we expect weak coupling between them to be mediated via commissural interneurons that cross the midline and could potentially transfer coordinating signals between premotor networks of the two hemisegments. This is supported by reports of premotor nonspiking neurons that process sensory signals coming from the contralateral side (Stein et al. 2006). In the mesothoracic ganglion of the stick insect, there are six dorsal and five ventral commissural tracts (Kittmann et al. 1991). Intracellular recording and identification of neurons that send their axons through those tracts may unravel the neural networks underlying weak intrasegmental coupling.

Conclusion

The stick insect walking system is a highly modular system. There are distinct oscillatory networks controlling the activity of single leg joints that need to be efficiently coordinated during walking. We show here that CPGs interact centrally at the premotor level and form a distributed coordinating network that is unable to generate the coordinating patterns expressed in vivo. However, this default coordinating scheme is susceptible to intersegmental and local sensory signals that shape its inherent pattern to produce behaviorally relevant motor output. Our data further support the notion that sensory input is more important for establishing coordination in slow walking animals.

ACKNOWLEDGMENTS

We thank the following colleagues who contributed to this work: N. Rosjat for helpful suggestions on a previous draft of the manuscript; A. Chockley for editing it; and M. Dübbert, J. Sydow, and H.-P. Bollhagen for providing excellent technical assistance.

GRANTS

This study was supported by the joint Bundesministerium für Bildung und Forschung/National Science Foundation Collaborative Research in Computational Neuroscience Project to A. Büschges, S. Daun (01GQ1412), and P. Holmes (DMS-1430077), entitled "Central pattern generators and reflexive feedback in insect locomotion: a cross-species study."

DISCLOSURES

No conflicts of interest, financial or otherwise, are declared by the authors.

AUTHOR CONTRIBUTIONS

C.M., P.H., A. Borgmann, S.D., and A. Bueschges conceived and designed research; C.M. performed experiments; C.M., T.B., and A. Bueschges analyzed data; C.M., T.B., P.H., A. Borgmann, S.D., and A. Bueschges interpreted results of experiments; C.M. prepared figures; C.M. and A. Bueschges drafted manuscript; C.M., P.H., S.D., and A. Bueschges edited and revised manuscript; C.M., T.B., P.H., A. Borgmann, S.D., and A. Bueschges approved final version of manuscript.

REFERENCES

Bässler U, Wegner U. Motor output of the denervated thoracic ventral nerve cord in the stick insect *Carausius morosus*. *J Exp Biol* 105: 127–145, 1983.

Bender JA, Simpson EM, Tietz BR, Daltorio KA, Quinn RD, Ritzmann RE. Kinematic and behavioral evidence for a distinction between trotting and ambling gaits in the cockroach *Blaberus discoidalis*. *J Exp Biol* 214: 2057–2064, 2011. doi:10.1242/jeb.056481.

Berendes V, Zill SN, Büschges A, Bockemühl T. Speed-dependent interplay between local pattern-generating activity and sensory signals during walking in *Drosophila*. *J Exp Biol* 219: 3781–3793, 2016. doi:10.1242/jeb.146720.

Berens P. CircStat: a MATLAB toolbox for circular statistics. *J Stat Softw* 31: 1–21, 2009. doi:10.18637/jss.v031.i10.

Biró Z, Hill RH, Grillner S. The activity of spinal commissural interneurons during fictive locomotion in the lamprey. *J Neurophysiol* 100: 716–722, 2008. doi:10.1152/jn.90206.2008.

Borgmann A, Hooper SL, Büschges A. Sensory feedback induced by front-leg stepping entrains the activity of central pattern generators in caudal segments of the stick insect walking system. *J Neurosci* 29: 2972–2983, 2009. doi:10.1523/JNEUROSCI.3155-08.2009.

Borgmann A, Scharstein H, Büschges A. Intersegmental coordination: influence of a single walking leg on the neighboring segments in the stick insect walking system. *J Neurophysiol* 98: 1685–1696, 2007. doi:10.1152/jn.00291.2007.

Burns MD. The control of walking in *Orthoptera*. I. Leg movements in normal walking. *J Exp Biol* 58: 45–58, 1973.

Büschges A. Role of local nonspiking interneurons in the generation of rhythmic motor activity in the stick insect. *J Neurobiol* 27: 488–512, 1995. doi:10.1002/neu.480270405.

Büschges A. Inhibitory synaptic drive patterns motoneuronal activity in rhythmic preparations of isolated thoracic ganglia in the stick insect. *Brain Res* 783: 262–271, 1998. doi:10.1016/S0006-8993(97)01370-X.

Büschges A, Akay T, Gabriel JP, Schmidt J. Organizing network action for locomotion: insights from studying insect walking. *Brain Res Rev* 57: 162–171, 2008. doi:10.1016/j.brainresrev.2007.06.028.

Büschges A, Schmitz J, Bässler U. Rhythmic patterns in the thoracic nerve cord of the stick insect induced by pilocarpine. *J Exp Biol* 198: 435–456, 1995.

Butt SJB, Kiehn O. Functional identification of interneurons responsible for left-right coordination of hindlimbs in mammals. *Neuron* 38: 953–963, 2003. doi:10.1016/S0896-6273(03)00353-2.

Couzin-Fuchs E, Kiemel T, Gal O, Ayali A, Holmes P. Intersegmental coupling and recovery from perturbations in freely running cockroaches. *J Exp Biol* 218: 285–297, 2015. doi:10.1242/jeb.112805.

Cruse H. The function of the legs in the free walking stick insect, *Carausius morosus*. *J Comp Physiol A Neuroethol Sens Neural Behav Physiol* 112: 235–262, 1976. doi:10.1007/BF00606541.

Cruse H. What mechanisms coordinate leg movement in walking arthropods? *Trends Neurosci* 13: 15–21, 1990. doi:10.1016/0166-2236(90)90057-H.

Cruse H, Knauth A. Coupling mechanisms betweeen the contralateral legs of a walking insect (*Carausisus morosus*). *J Exp Biol* 144: 199–213, 1989.

Cruse H, Saxler G. Oscillations of force in the standing legs of a walking insect (*Carausius morosus*). *Biol Cybern* 36: 159–163, 1980. doi:10.1007/BF00365770.

Dallmann CJ, Dürr V, Schmitz J. Joint torques in a freely walking insect reveal distinct functions of leg joints in propulsion and posture control. *Proc Biol Sci* 283: 20151708, 2016. doi:10.1098/rspb.2015.1708.

David I, Holmes P, Ayali A. Endogenous rhythm and pattern-generating circuit interactions in cockroach motor centres. *Biol Open* 5: 1229–1240, 2016. doi:10.1242/bio.018705.

Dean J. Leg coordination in the stick insect *Carausius morosus*: effects of cutting thoracic connectives. *J Exp Biol* 145: 103–131, 1989.

Dürr V, Schmitz J, Cruse H. Behaviour-based modelling of hexapod locomotion: linking biology and technical application. *Arthropod Struct Dev* 33: 237–250, 2004. doi:10.1016/j.asd.2004.05.004.

Fuchs E, Holmes P, David I, Ayali A. Proprioceptive feedback reinforces centrally generated stepping patterns in the cockroach. *J Exp Biol* 215: 1884–1891, 2012. doi:10.1242/jeb.067488.

Fuchs E, Holmes P, Kiemel T, Ayali A. Intersegmental coordination of cockroach locomotion: adaptive control of centrally coupled pattern generator circuits. *Front Neural Circuits* 4: 125, 2011. doi:10.3389/fncir.2010.00125.

Goldammer J, Büschges A, Schmidt J. Motoneurons, DUM cells, and sensory neurons in an insect thoracic ganglion: a tracing study in the stick insect *Carausius morosus*. *J Comp Neurol* 520: 230–257, 2012. doi:10.1002/cne.22676.

Grabowska M, Godlewska E, Schmidt J, Daun-Gruhn S. Quadrupedal gaits in hexapod animals—inter-leg coordination in free-walking adult stick insects. *J Exp Biol* 215: 4255–4266, 2012. doi:10.1242/jeb.073643.

Graham D. Influence of coxa-thorax joint receptors on retractor motor output during walking in *Carausius morosus*. *J Exp Biol* 114: 131–139, 1985.

Grillner S. The motor infrastructure: from ion channels to neuronal networks. *Nat Rev Neurosci* 4: 573–586, 2003. doi:10.1038/nrn1137.

Hägglund M, Dougherty KJ, Borgius L, Itohara S, Iwasato T, Kiehn O. Optogenetic dissection reveals multiple rhythmogenic modules underlying locomotion. *Proc Natl Acad Sci USA* 110: 11589–11594, 2013. doi:10.1073/pnas.1304365110.

Hughes GM. The co-ordination of insect movements. *J Exp Biol* 29: 267–285, 1952.

Johnston RM, Levine RB. Locomotory behavior in the hawkmoth *Manduca sexta*: kinematic and electromyographic analyses of the thoracic legs in larvae and adults. *J Exp Biol* 199: 759–774, 1996.

Johnston RM, Levine RB. Thoracic leg motoneurons in the isolated CNS of adult *Manduca* produce patterned activity in response to pilocarpine, which is distinct from that produced in larvae. *Invert Neurosci* 4: 175–192, 2002. doi:10.1007/s10158-002-0019-4.

Katz PS, Hooper SL. Invertebrate central pattern generators. In: *Invertebrate Neurobiology*, edited by Norrth G, Greenspan RJ. Cold Spring Harbor, NY: Cold Spring Harbor Laboratory Press, 2007.

Kittmann R, Dean J, Schmitz J. An atlas of the thoracic ganglia in the stick insect, *Carausius morosus*. *Philos Trans R Soc Lond B Biol Sci* 331: 101–121, 1991. doi:10.1098/rstb.1991.0002.

Knebel D, Ayali A, Pflüger HJ, Rillich J. Rigidity and flexibility: the central basis of inter-leg coordination in the locust. *Front Neural Circuits* 10: 112, 2017. doi:10.3389/fncir.2016.00112.

Kralemann B, Cimponeriu L, Rosenblum M, Pikovsky A, Mrowka R. Phase dynamics of coupled oscillators reconstructed from data. *Phys Rev E Stat Nonlin Soft Matter Phys* 77: 066205, 2008. doi:10.1103/PhysRevE.77.066205.

Ludwar BC, Göritz ML, Schmidt J. Intersegmental coordination of walking movements in stick insects. *J Neurophysiol* 93: 1255–1265, 2005. doi:10.1152/jn.00727.2004.

Marder E, Bucher D. Central pattern generators and the control of rhythmic movements. *Curr Biol* 11: R986–R996, 2001. doi:10.1016/S0960-9822(01)00581-4.

Marder E, Calabrese RL. Principles of rhythmic motor pattern generation. *Physiol Rev* 76: 687–717, 1996.

Mendes CS, Bartos I, Akay T, Márka S, Mann RS. Quantification of gait parameters in freely walking wild type and sensory deprived Drosophila melanogaster. *Elife* 2: e00231, 2013. doi:10.7554/eLife.00231.

Orlovsky GN, Deliagina TG, Grillner S. *Neuronal Control of Locomotion*. Oxford: Oxford University Press, 1999. doi:10.1093/acprof:oso/9780198524052.001.0001.

Pikovsky A, Rosenblum M, Kurths J. *Synchronization: A Universal Concept in Nonlinear Sciences*. New York: Cambridge University Press, 2001. doi:10.1017/CBO9780511755743.

Quinlan KA, Kiehn O. Segmental, synaptic actions of commissural interneurons in the mouse spinal cord. *J Neurosci* 27: 6521–6530, 2007. doi:10.1523/JNEUROSCI.1618-07.2007.

Rosenbaum P, Wosnitza A, Büschges A, Gruhn M. Activity patterns and timing of muscle activity in the forward walking and backward walking stick insect *Carausius morosus*. *J Neurophysiol* 104: 1681–1695, 2010. doi:10.1152/jn.00362.2010.

Ryckebusch S, Laurent G. Rhythmic patterns evoked in locust leg motor neurons by the muscarinic agonist pilocarpine. *J Neurophysiol* 69: 1583–1595, 1993.

Ryckebusch S, Laurent G. Interactions between segmental leg central pattern generators during fictive rhythms in the locust. *J Neurophysiol* 72: 2771–2785, 1994.

Sakurai A, Katz PS. The central pattern generator underlying swimming in Dendronotus iris: a simple half-center network oscillator with a twist. *J Neurophysiol* 116: 1728–1742, 2016. doi:10.1152/jn.00150.2016.

Schilling M, Hoinville T, Schmitz J, Cruse H. Walknet, a bio-inspired controller for hexapod walking. *Biol Cybern* 107: 397–419, 2013. doi:10.1007/s00422-013-0563-5.

Schmitz J, Büschges A, Delcomyn F. An improved electrode design for en passant recording from small nerves. *Comp Biochem Physiol A* 91: 769–772, 1988. doi:10.1016/0300-9629(88)90963-2.

Schütz C, Dürr V. Active tactile exploration for adaptive locomotion in the stick insect. *Philos Trans R Soc Lond B Biol Sci* 366: 2996–3005, 2011. doi:10.1098/rstb.2011.0126.

Smarandache-Wellmann CR. Arthropod neurons and nervous system. *Curr Biol* 26: R960–R965, 2016. doi:10.1016/j.cub.2016.07.063.

Smith JC, Abdala APL, Borgmann A, Rybak IA, Paton JFR. Brainstem respiratory networks: building blocks and microcircuits. *Trends Neurosci* 36: 152–162, 2013. doi:10.1016/j.tins.2012.11.004.

Stein W, Büschges A, Bässler U. Intersegmental transfer of sensory signals in the stick insect leg muscle control system. *J Neurobiol* 66: 1253–1269, 2006. doi:10.1002/neu.20285.

Talpalar AE, Bouvier J, Borgius L, Fortin G, Pierani A, Kiehn O. Dual-mode operation of neuronal networks involved in left-right alternation. *Nature* 500: 85–88, 2013. doi:10.1038/nature12286.

Tass P, Rosenblum MG, Weule J, Kurths J, Pikovsky A, Volkmann J, Schnitzler A, Freund H-J. Detection of n:m phase locking from noisy data: application to magnetoencephalography. *Phys Rev Lett* 81: 3291–3294, 1998. doi:10.1103/PhysRevLett.81.3291.

Trimmer BA. Current excitement from insect muscarinic receptors. *Trends Neurosci* 18: 104–111, 1995. doi:10.1016/0166-2236(95)80032-W.

Wendler G. [Walking and standing of the stick insect *Carausius morosus*: sensory bristles at the leg joints as parts of closed-loop control circuits]. *Z Vgl Physiol* 48: 198–250, 1964. doi:10.1007/BF00297860.

Wendler G. The co-ordination of walking movements in arthropods. *Symp Soc Exp Biol* 20: 229–249, 1966.

Wilson DM. Insect walking. *Annu Rev Entomol* 11: 103–122, 1966. doi:10.1146/annurev.en.11.010166.000535.

Wolf H, Ronacher B, Reichert H. Patterned synaptic drive to locust flight motoneurons after hemisection of thoracic ganglia. *J Comp Physiol A Neuroethol Sens Neural Behav Physiol* 163: 761–769, 1988. doi:10.1007/BF00604053.

Wosnitza A, Bockemühl T, Dübbert M, Scholz H, Büschges A. Inter-leg coordination in the control of walking speed in *Drosophila*. *J Exp Biol* 216: 480–491, 2013. doi:10.1242/jeb.078139.